



1 **Measurements of the OH radical yield from the ozonolysis of** 2 **biogenic alkenes: A potential interference with laser-induced** 3 **fluorescence measurements of ambient OH**

4 Pamela Rickly¹ and Philip S. Stevens^{1,2}

5 ¹School of Public and Environmental Affairs, Indiana University, Bloomington, IN USA

6 ²Department of Chemistry, Indiana University, Bloomington, IN USA

7 *Correspondence to:* Philip S. Stevens (pstevens@indiana.edu)

8 **Abstract.** Reactions of the hydroxyl radical (OH) play a central role in the chemistry of the atmosphere, and
9 measurements of its concentration can provide a rigorous test of our understanding of atmospheric oxidation.
10 Several recent studies have shown large discrepancies between measured and modeled OH concentrations in
11 forested areas impacted by emissions of biogenic volatile organic compounds (BVOCs), where modeled
12 concentrations were significantly lower than measurements. A potential reason for some of these discrepancies
13 involves interferences associated with the measurement of OH using the Laser-Induced Fluorescence -
14 Fluorescence Assay with Gas Expansion (LIF-FAGE) technique in these environments. In this study, a turbulent
15 flow reactor operating at atmospheric pressure was coupled to a LIF-FAGE cell and the OH signal produced from
16 the ozonolysis of several BVOCs was measured. To distinguish between OH produced from the ozonolysis
17 reactions and any OH artefact produced inside the LIF-FAGE cell, an external chemical scrubbing technique was
18 used, allowing for the direct measurement of any interference. An interference under high ozone and BVOC
19 concentrations was observed that was not laser generated and was independent of the ozonolysis reaction time.
20 Addition of acetic acid to the reactor eliminated the interference, suggesting that the source of the interference in
21 these experiments involved the decomposition of stabilized Criegee intermediates inside the FAGE detection cell.



1 1. Introduction

2 The hydroxyl radical (OH) plays an important role in the chemistry of the atmosphere. OH initiates the oxidation
3 of volatile organic compounds (VOCs) which in the presence of nitrogen oxides (NO_x) can lead to the production
4 of ozone and secondary organic aerosols, the primary components of photochemical smog. Because of its high
5 reactivity, measurements of OH can provide a rigorous test of our understanding of the fast radical chemistry in
6 the atmosphere. However, several field campaigns have identified significant discrepancies between measured
7 and modeled OH concentrations, especially in low NO_x forested environments (Rohrer et al., 2014). For example,
8 Ren et al. (2008) found that OH concentrations were well predicted by models to within their combined estimated
9 uncertainty when mixing ratios of isoprene were less than approximately 500 pptv, but measurements acquired in
10 areas with higher mixing ratios of isoprene showed observed OH concentrations that were 3-5 times larger than
11 model predictions. Similarly, measurements in a northern Michigan forest found daytime OH concentrations
12 approximately three times larger and nighttime concentrations 3-10 times larger than model predictions (Tan et
13 al., 2001; Faloon et al., 2001). Aircraft measurements over the Amazon rainforest found OH concentrations to
14 be 40-80% larger than model predictions (Lelieveld et al., 2008). Similarly, measurements of OH concentrations
15 under high mixing ratios of isoprene in the Pearl River Delta, China were 3-5 times larger than model predictions
16 (Hofzumahaus et al., 2009).

17 Most of these measurements were done using the Laser-Induced Fluorescence – Fluorescence Assay by
18 Gas Expansion (LIF-FAGE) technique. In this technique, ambient air is sampled through an inlet at low pressure,
19 enhancing the OH fluorescence lifetime and allowing temporal filtering of the OH fluorescence from laser scatter
20 (Heard and Pilling, 2003). Fluorescence from OH radicals is distinguished from background scatter and broadband
21 fluorescence through spectral modulation of the laser wavelength. Previous laboratory tests demonstrated that the
22 technique was free from interferences from several species, including spectral interferences from naphthalene,
23 sulfur dioxide, and formaldehyde as well as chemical interferences from high concentrations of H₂O₂, HONO,
24 SO₂, HNO₃, several alcohols and alkanes, propene, and isoprene (Ren et al., 2004). Mixtures of ozone with ethene,
25 propylene and isoprene did not result in any significant signal, suggesting that the ozonolysis of these compounds
26 did not produce an interference in their instrument, although small interferences were observed with addition of
27 high amounts of ozone and acetone that would be insignificant under ambient conditions (Ren et al., 2004).
28 Measurements of OH in the SAPHIR chamber by both an LIF-FAGE instrument and a differential optical
29 absorption spectroscopy (DOAS) instrument were in excellent agreement, suggesting that measurements of OH
30 using the LIF-FAGE instrument were free from artifacts (Schlossler et al., 2007). A subsequent intercomparison
31 inside the SAPHIR chamber found that measurements from several different LIF-FAGE instruments under a



1 variety of conditions agreed with each other to within the calibration accuracies of the instruments (Schlosser et
2 al., 2009). No interferences were detected under varying concentrations of O₃, H₂O, NO_x and peroxy radicals, and
3 measurements of OH during the ozonolysis of various mixing ratios of pent-1-ene (6-25 ppb) and trans-2-butene
4 (200 ppb) in approximately 100 ppb of ozone also did not reveal a significant interference (Schlosser et al., 2009).
5 In contrast, Hard et al. (2002) observed an interference in their LIF-FAGE instrument during calibrations using
6 the ozonolysis of trans-2-butene under high mixing ratios of both ozone (up to 28 ppm) and trans-2-butene (greater
7 than 12 ppb). Tests suggested that the interference was not laser generated, and disappeared in air containing 1%
8 water vapor. They suggested that the interference may be due to the dissociation of an intermediate in the
9 ozonolysis mechanism that produces OH in the low-pressure cell of their FAGE instrument (Hard et al., 2002).

10 Recently, Mao et al. (2012) discovered a significant interference associated with their LIF-FAGE
11 measurements of OH in a northern California forest. Using a chemical scavenger to remove ambient OH before
12 air enters the inlet, they found that subsequent spectral modulation revealed a significant amount of internally
13 generated OH from an unknown interference. Measurements using only spectral modulation of the laser
14 wavelength were greater than the measurements when the interference measured using the chemical scavenger
15 was subtracted, and the latter measurements were in better agreement with model predictions (Mao et al., 2012).
16 Similar results were observed by Novelli et al. (2014a) who measured ambient OH concentrations in several forest
17 environments using an external chemical scavenger technique. They found that OH generated inside their
18 detection cell comprised 30-80% of the daytime signal observed using spectral modulation and 60-100% of the
19 signal observed at night. Subtracting the interference from the ambient signal resulted in OH concentrations that
20 were in good agreement with model simulations.

21 Mao et al. (2012) found that the interference increased with both temperature and measured OH
22 reactivity, suggesting that the interference was related to biogenic emissions in this environment, perhaps the
23 result of BVOC oxidation products entering the sampling cell of the LIF-FAGE instrument which subsequently
24 undergo further reactions and/or decomposition producing the additional OH signal. Novelli et al. (2016) also
25 found that the interference appeared to correlate with temperature similar to the temperature dependence of terpene
26 emissions and was also correlated with the measured ozone concentrations. They concluded that one possible
27 contributor to their interference was the decomposition of stabilized Criegee intermediates inside their instrument.
28 Previous laboratory experiments have shown that BVOC ozonolysis intermediates, such as Criegee intermediates
29 and vinyl hydroperoxides, are likely to promptly decompose to produce OH at low pressures (Kroll et al.,
30 2001a,b). As a result of the large pressure and temperature gradients which occur as the sample enters the FAGE
31 detection cell, the dissociation pathway of these intermediate species may be favored, leading to additional OH



1 production. Recently, Fuchs et al. (2016) performed laboratory and chamber experiments to determine whether
2 the ozonolysis of alkenes produced an OH artifact in their LIF-FAGE instrument. They found that under reactant
3 concentrations that were orders of magnitude greater than ambient, the ozonolysis of propene, α -pinene, limonene,
4 and isoprene produced a detectable interference in their instrument that increased with the turnover rate of the
5 reaction. Extrapolating their results to ambient concentrations of ozone and alkenes would suggest that the
6 ozonolysis of these compounds would not produce a detectable interference in their instrument under ambient
7 conditions (Fuchs et al., 2016).

8 The goal of this work is to determine whether intermediates or products in the ozonolysis of various
9 biogenic alkenes can lead to an interference with OH measurements using the Indiana University LIF-FAGE
10 instrument. These experiments focus on the ozonolysis of several biogenic alkenes, including α -pinene, β -pinene,
11 ocimene, isoprene, and 2-methyl-3-buten-2-ol (MBO). Measurements of the interference as a function of various
12 instrumental parameters are also provided in an attempt to identify possible sources of the interference and ways
13 it could be minimized.

14 2. Experimental Section

15 The ozonolysis experiments were performed using an atmospheric pressure turbulent flow tube similar to that
16 used for ambient measurements of total OH reactivity (Hansen et al., 2014). The 1 m long and 5 cm diameter flow
17 tube was positioned perpendicular to the IU-FAGE detection cell so that the flow would not interfere with the
18 external OH scavenging measurement (section 2.2) (Fig. 1). A Teflon adaptor attached at one end of the flow tube
19 supported the injector, a 1 m stainless steel tube with a 1.25 cm diameter. This injector allowed for the introduction
20 of ozone produced from an ozone generator (Enaly) to the system and could be moved throughout the flow tube
21 to permit varying reaction times between approximately 100 and 420 ms. Attached to the end of the injector was
22 a turbulizer used to increase mixing of the reagents at the start of the reaction. A flow of nitrogen of 180 SLPM
23 created a turbulent flow with a Reynolds number of approximately 3750. Ozone concentrations were varied
24 between approximately 1 and 3 ppm (2×10^{13} - 7×10^{13} molecules cm^{-3}) and measured using a Teledyne Photometric
25 Ozone Analyzer (model 400E).

26 BVOC concentrations were introduced into the flow tube by bubbling N_2 through the liquid compound
27 sending the vapor into the reactor. The concentration of the BVOC was estimated from its equilibrium vapor
28 pressure and accounting for dilution into the main flow. Several alkene concentrations were used for each



1 experiment, with approximate concentrations of 2×10^{11} to 4×10^{13} molecules cm^{-3} for α -pinene, 1×10^{11} to 4×10^{13}
2 molecules cm^{-3} for β -pinene, and 9×10^{10} to 5×10^{13} molecules cm^{-3} for ocimene.

3 2.1 Detection of OH Radicals

4 OH radicals were measured using the IU-FAGE instrument, in which ambient air is pulled through either a 0.6 or
5 1 mm diameter nozzle and expanded to a total pressure of approximately 4-9 Torr resulting in a total flow rate of
6 approximately 8-10 SLPM (Dusanter et al., 2008; 2009; Griffith et al., 2013; 2016). Previous field measurements
7 using the IU-FAGE instrument have incorporated a cylindrical inlet (5 cm diameter, 14 cm long) attached to the
8 main detection block resulting in a total distance of approximately 20 cm from the nozzle to the detection volume
9 (Fig. 2). These previous field measurements have utilized both the 0.6 mm nozzle (Griffith et al., 2016) and the 1
10 mm nozzle (Dusanter et al., 2009; Griffith et al., 2013), and the experiments presented here have attempted to
11 reproduce these instrument configurations.

12 The original IU-FAGE laser system used in this study consisted of a Spectra Physics Navigator II
13 YHP40-532Q diode-pumped Nd:YAG laser that produces approximately 5.5W of radiation at 532 nm at a
14 repetition rate of 5 kHz. This laser pumped a Lambda Physik Scanmate 1 dye laser (Rhodamine 640, 0.25 g L^{-1}
15 in isopropanol) that produced tunable radiation around 616 nm, which was frequency doubled to generate 2 to 20
16 mW of radiation at 308 nm. This laser system was recently replaced with a Spectra Physics Navigator II YHP40-
17 532Q that produces approximately 8 W of radiation at 532 nm at a repetition rate of 10 kHz that pumps a Sirah
18 Credo Dye laser (255 mg/L of Rhodamine 610 and 80 mg/L of Rhodamine 101 in ethanol), resulting in 40 to 100
19 mW of radiation at 308 nm.

20 After exiting the dye laser, the beam is focused onto a 12 m optical fiber to transmit the radiation to the
21 sampling cell where it crosses the expanded air perpendicular to the flow approximately 24 times in a multipass
22 White cell configuration (Fig. 2). The OH molecule is excited and detected using the $A^2\Sigma^+ (v'=0) \leftarrow X^2\Pi_i (v''=$
23 $0)$ transition near 308 nm. A reference cell where OH is produced by thermal dissociation of water vapor is used
24 to ensure that the laser is tuned on-line and off-line of the OH transition to measure the net fluorescence signal.
25 The OH fluorescence is detected by a gated microchannel plate detector (Hamamatsu R5916U-52) and the
26 resulting signal is sent through a preamplifier (Stanford Research SR445) and a photon counter (Stanford Research
27 SRS 400). The detector is switched off during the laser pulse through the use of electronic gating, allowing the
28 OH fluorescence to be temporally filtered from laser scatter. Each offline measurement is recorded for
29 approximately 10 seconds and is averaged and subtracted from the online measurement, averaged for



1 approximately 20 seconds. These measurements are recorded for at least 5 cycles per ozone concentration once
2 the OH concentration has stabilized.

3 The sensitivity of the IU LIF-FAGE instrument was calibrated using the UV-water photolysis technique
4 where water vapor is photolyzed to produce known amounts of OH (Dusanter et al., 2008). In these experiments,
5 calibrations were performed under the conditions of the experiments using N₂, resulting in larger calibration
6 factors compared to ambient air due to fluorescence quenching by oxygen. The N₂ calibration factors were
7 determined for various instrumental parameters including three cell pressures (4, 7, and 9 Torr), the two nozzle
8 diameters (0.6 mm and 1 mm), and three inlet lengths (4.5 cm, 14 cm, and 23.5 cm) (Fig. S1). Both nozzle
9 diameters showed similar sensitivities that decreased as the pressure increased due to increased collisional
10 quenching of the OH fluorescence. The calibration factor was also sensitive to the length of the inlet where the
11 ambient air enters the cell and where the OH fluorescence occurs in the detection axis, with the sensitivity
12 decreasing with the increasing inlet length likely due to increased loss of OH radicals on the interior walls of the
13 inlet. For these experiments, the limit of detection was between approximately 4×10^5 - 3×10^6 molecules cm⁻³
14 (S/N=1, 10 min integration) depending on the inlet configuration, flow rate, and pressure inside the FAGE
15 detection cell, with the lowest value corresponding to the shortest inlet and lowest pressure, and the highest value
16 corresponding to the longest inlet and highest pressure.

17 2.2 Measuring the OH Interference

18 The OH interference was measured using a chemical titration scheme in which perfluoropropylene (C₃F₆, 1% in
19 N₂, Matheson) was added through a circular injector surrounding the detection inlet to chemically remove external
20 OH (Griffith et al., 2016) (Fig. 2). Measurements of OH concentrations using spectral modulation with C₃F₆ added
21 externally reflect OH radicals generated inside the detection cell. C₃F₆ was used because it reacts quickly with
22 OH while also having a negligible optical absorption around 308 nm (Mao et al. 2012). To determine the flow of
23 C₃F₆ to be used, OH was produced from the photolysis of ambient air using a mercury penlamp placed in front of
24 the IU LIF-FAGE inlet (Fig. S2). Once a constant OH signal was established, C₃F₆ was added at varying flows to
25 determine the flow that depleted $\geq 90\%$ of the external OH signal (a flow of approximately 3-5 sccm). To ensure
26 that this flow of C₃F₆ did not titrate OH radicals produced inside the detection cell, a penlamp was placed inside
27 the detection cell directly behind the inlet to generate OH radicals internally. The same external C₃F₆ flow was
28 again introduced to ensure that the concentration of C₃F₆ after expansion into the detection cell was not high
29 enough to titrate any internally generated OH.



1 By applying this C₃F₆ titration method to the alkene ozonolysis experiments, any OH produced in the
2 flow tube was expected to be removed. Any OH that was measured using spectral modulation after C₃F₆ addition
3 would, therefore, be an interference generated internally. Subtraction of this interference from the measurement
4 acquired before C₃F₆ addition should reflect the steady-state OH concentration generated in the flow tube, which
5 can then be compared to literature values of the OH yield for the ozonolysis of these alkenes.

6 3. Results and Discussion

7 3.1 Ozonolysis experiments

8 The interference tests were performed during the alkene ozonolysis experiments with a reaction time in the flow
9 tube of approximately 420 ms, a reaction time longer than that required for the system to reach steady-state
10 (approximately 20 ms), and the results are shown in Figs. 3 and 4. In these figures, the open symbols are the
11 measured OH concentration produced from the ozonolysis reaction without addition of C₃F₆ (W/int), and the filled
12 symbols represent the OH signal after the signal measured with C₃F₆ addition is removed (W/O int) using the 0.6
13 mm nozzle. The expected steady-state OH concentrations based on previous measurements of the OH yield for
14 each compound are also shown in each figure by the solid line, calculated using the following equation:

$$15 \quad [\text{OH}]_{ss} = \frac{k_{O_3} \alpha [\text{O}_3] [\text{alkene}]}{k_{OH} [\text{alkene}] + k_{OH+O_3} [\text{O}_3] + k_{wall}} \approx \frac{k_{O_3} \alpha [\text{O}_3]}{k_{OH}} \quad (1)$$

16 In this equation, k_{O_3} is the rate constant for the O₃ + alkene reaction with an OH yield of α , k_{OH} is the rate constant
17 for the OH + alkene reaction, k_{OH+O_3} is the rate constant for the OH + O₃ reaction, and k_{wall} is the first-order loss
18 of OH on the walls of the reactor, measured as before (Hansen et al., 2014). Rate constants for the OH and O₃
19 reactions were obtained from recommendations by Atkinson (1997) and Atkinson et al. (2006). For these
20 calculations, the loss of OH from reaction with ozone as well as wall loss of OH were neglected, as they were
21 much smaller than loss of OH due to reaction with the alkenes due to the high concentration of alkenes used in
22 these experiments.

23 As illustrated in Fig. 3, the measured OH concentration from the ozonolysis of α -pinene without C₃F₆
24 addition is consistently greater than the measurements after the interference is subtracted, indicating that a
25 significant concentration of OH is being produced inside the detection cell. Experiments without α -pinene in
26 which ozone alone was sampled by the detection cell showed a negligible OH signal, suggesting that the
27 interference was related to the presence of both the alkene and ozone. The observed interference measured with



the addition of C_3F_6 accounted for approximately 40-60% of the observed signal in the absence of C_3F_6 . When the measured interference was subtracted from the overall signal, the resulting OH concentrations were in reasonable agreement with the OH yield expected from α -pinene ozonolysis producing an OH yield of approximately 0.81 ± 0.10 , determined from the slope of the plot of the OH concentration versus ozone concentration, in good agreement with the value of 0.76 ± 0.11 as reported by Chew and Atkinson (1996) and the value of 0.91 ± 0.23 reported by Siese et al. (2001).

The measured interference appeared to depend on the length of the inlet, with the greatest interference observed with the longest inlet (Fig. 3). Similar results were observed with the use of the 1 mm nozzle diameter (Fig. S3). These results are comparable to that observed by Fuchs et al. (2016), who found that the interference from the ozonolysis of α -pinene, limonene and isoprene also increased with the length of the inlet in their FAGE instrument. But while the inlet length appears to exhibit a trend in the OH interference, the cell pressure did not appear to significantly impact the level of the interference except at the longest inlet length. These results are in contrast to the results of Fuchs et al. (2016), who found that the interference in their instrument decreased with cell pressure, although the effect was greater with the longer inlet. The changing cell pressures in these experiments were obtained by changing the pumping speed, which likely impacts the velocity and residence time of the airstream inside the detection cell. This suggests that increasing the reaction time for the shortest inlets does not significantly impact the interference, while increasing the reaction time for the longest inlet does increase the interference. However, at the longest inlet length, the increased reaction time likely also leads to increased collisions with the interior surfaces of the detection cell, which could also lead to increased dissociation and production of OH. These results appear to be independent of the α -pinene concentration (Fig. 4, top) as the level of the interference is similar for α -pinene concentrations between approximately 1 and 4×10^{13} molecules cm^{-3} .

The results from the ozonolysis of β -pinene are also shown in Fig. 4 (middle). Similar to that observed for the ozonolysis of α -pinene, the observed interference measured with the addition of C_3F_6 accounted for approximately 40% of the observed signal in the absence of C_3F_6 . When the measured interference was subtracted from the overall signal, the measured OH concentrations results in an overall OH yield of approximately 0.40 ± 0.01 , which is in good agreement with the value reported by Atkinson et al. (1992) of 0.35 ± 0.05 . Similar to that observed for the ozonolysis of α -pinene, the interference and the observed OH yield did not significantly increase with increasing concentrations of β -pinene.

Measurements of the concentration of OH produced from the ozonolysis of various concentrations of ocimene are also shown in Fig. 4 (bottom). In contrast to the ozonolysis of α - and β -pinene, the interference and

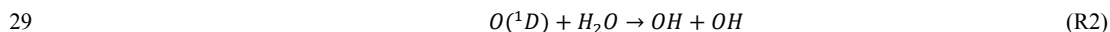
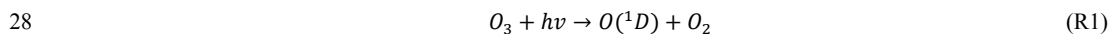


1 the observed OH yield appear to increase with increasing ocimene concentration. At ocimene concentrations of
2 approximately 4×10^{11} molecules cm^{-3} , an OH yield of approximately 0.28 ± 0.02 was measured. However, the
3 apparent OH yield increased to a yield of 1.0 ± 0.03 at the highest ocimene concentration (approximately 5×10^{13}
4 molecules cm^{-3}). Additional ocimene ozonolysis experiments were performed using the two nozzle diameters and
5 three inlet lengths with the results shown in Fig. S4. These results show that the measured OH yield from ocimene
6 ozonolysis after subtracting the interference is only consistent with the results of Aschmann et al. (2002) of 0.55
7 ± 0.9 for an ocimene concentration of approximately 1×10^{13} molecules cm^{-3} . The increase in the apparent OH
8 yield and interference as the concentration of ocimene was increased may be due to the additional ozonolysis of
9 the reaction products, as the products of ocimene ozonolysis are likely unsaturated. The higher ocimene
10 concentrations would lead to increased concentrations of reaction products, which in turn could also contribute to
11 the measured interference and OH yield. Additional experiments are needed in order to better quantify the OH
12 yield from the ozonolysis of ocimene.

13 In contrast to the measurements involving α -pinene, β -pinene, and ocimene, similar ozonolysis
14 experiments involving isoprene and MBO did not produce a detectable OH signal or interference under the highest
15 ozone and alkene concentrations. These results may reflect the higher reactivity of α -pinene, β -pinene, and
16 ocimene with ozone compared to that of isoprene and MBO under the conditions of these experiments, and do not
17 rule out the possibility of an interference from the ozonolysis of these compounds. The lower reactivity of isoprene
18 and MBO with ozone would likely require longer reaction times or higher concentrations of ozone and/or alkenes
19 to establish steady-state OH concentrations above the detection limit of the instrument in these experiments. Fuchs
20 et al. (2016) did find a significant unexpected OH signal in laboratory under very high concentrations of isoprene
21 and a reaction time on the order of 1 s. Future experiments will involve higher concentrations of ozone, isoprene
22 and MBO and/or longer reaction times to increase the ozonolysis rate for these reactions and to determine the
23 potential magnitude of the interference from isoprene and MBO in the IU-FAGE instrument.

24 3.2 Interference measurements as a function of laser power, ozone, and ozonolysis reaction time

25 A potential interference with the detection of OH radicals by laser-induced fluorescence is the production of OH
26 through photolysis of ozone by the laser, with the resulting excited oxygen atoms reacting with ambient water
27 vapor to produce OH (reactions R1 and R2) (Stevens et al., 1994; Ren et al., 2004):





1 The resulting OH signal from this two-photon process would display a quadratic dependence on laser power. One
2 possible source of the interference observed in the ozonolysis experiments could be $O(^1D)$ produced from the
3 photolysis of ozone by the laser reacting with the alkene leading to the production of OH radicals through a
4 hydrogen abstraction mechanism. The OH signal from this two-photon process would also display a quadratic
5 dependence on laser power.

6 To confirm that laser generated OH was not occurring within this instrument and was not the source of
7 the interference, experiments were conducted over a wide range of laser powers (0.6-12 mW) to determine
8 whether the observed interference displayed a dependence on laser power consistent with a laser-generated
9 mechanism. Fig. 5 (top) shows the measurements of the OH concentration with and without the interference for
10 the ozonolysis of ocimene as a function of laser power. These experiments were done under dry conditions to
11 minimize potential laser-generated interferences from reactions R1 and R2. Because the OH concentration
12 remained relatively stable over the range of laser powers used in these experiments, there is no indication that the
13 interference was due to a laser-generated mechanism. These results are similar to that found by Novelli et al.
14 (2014a) and Fuchs et al. (2016).

15 A plot of the interference at different ozone concentrations is also shown in Fig. 5 (middle) for the
16 ozonolysis of α -pinene as an example. Comparing the measured interference for each inlet length and ozone
17 concentration shows a trend in which the interference appears to increase with increasing ozone concentration,
18 with the greatest increase occurring with the longest inlet. Similar to the results of Fuchs et al. (2016), the observed
19 interference appears to increase with the overall ozonolysis turnover time (Fig. 6). Although the magnitude of the
20 interference observed here is greater due to the greater turnover rates used in these experiments, the slope of the
21 observed interference as a function of the turnover rate appears to be similar to that observed by Fuchs et al.
22 (2016). However, this agreement may be fortuitous, as differences in the design of the individual instruments may
23 impact the level of the interference.

24 The interference signals from the ozonolysis of α -pinene expressed as a percentage of the total OH signal
25 at several ozone concentrations and cell pressures for the short, medium, and long inlets are shown in Fig. S5. On
26 average, the percent interference was similar for ozone mixing ratios between 1-3 ppm, with values of
27 approximately $45 \pm 3\%$, $37 \pm 8\%$, and $58 \pm 8\%$ for the short, medium, and long inlets, respectively for the 1 mm
28 nozzle, and approximately $54 \pm 7\%$, $50 \pm 13\%$, and $65 \pm 11\%$ for the short, medium, and long inlets, respectively
29 for the 0.6 mm nozzle. Similar results were observed for the ozonolysis of ocimene (Fig. S6), with average percent
30 interferences of $75 \pm 1\%$, $89 \pm 2\%$, and $83 \pm 2\%$, for the short, medium, and long inlets respectively with the 1



1 mm nozzle, and $78 \pm 1\%$, $89 \pm 1\%$, and $86 \pm 2\%$, for the short, medium, and long inlets, respectively with the 0.6
2 mm nozzle (Fig. S6).

3 The interference was also measured over varying reaction times within the flow tube, and an example of
4 the results is shown in Fig. 5 (bottom). The results appear to indicate that the level of interference does not depend
5 on the ozonolysis reaction time, suggesting that the interference is not due to a stable oxidation product but may
6 be due to a steady-state intermediate in the ozonolysis mechanism, as an interference due to stable oxidation
7 products would likely increase with reaction time. The consistency of the measured interference relative to the
8 OH concentration produced from the ozonolysis mechanism may suggest that the source of the interference is
9 related to the source of OH, such as the Criegee intermediate.

10 3.3 Stabilized Criegee intermediates as a source of the interference

11 The ozonolysis of alkenes involves the addition of ozone to the double bond, forming a primary ozonide
12 which quickly decomposes to an excited Criegee intermediate and a carbonyl compound. Depending on its
13 structure, the excited Criegee intermediate can either decompose to form an OH radical, or can be stabilized by
14 collisions forming a stabilized Criegee intermediate (SCI), which can also thermally dissociate into OH at long
15 reaction times. At short reaction times, the excited Criegee intermediate is in steady-state with respect to
16 dissociation and stabilization, resulting in OH concentrations that are generally independent of reaction time, but
17 increase at longer reaction times due to the additional OH production from SCIs (Kroll et al., 2001b).

18 The time dependence of the observed interference in these experiments, with the interference appearing
19 to be independent of reaction time except under the longest reaction time, at first appears to be consistent with a
20 mechanism that involves the formation of excited Criegee radicals inside the FAGE detection cell. However, it is
21 unlikely that excited Criegee intermediates could be produced directly from alkene ozonolysis inside the IU-
22 FAGE detection cell as the decrease in reactant concentrations from the expansion to low pressure leads to
23 turnover rates that are approximately two orders of magnitude smaller than that shown in Fig. 6. For the ozonolysis
24 of α -pinene, a reaction time of approximately 0.5-1 s would be required to internally produce the observed OH
25 signals in these experiments, which is much longer than the reaction time inside the detection cell (on the order
26 of 1-2 ms). The lower pressure in the FAGE detection cell may result in higher yields of OH due to the lower rate
27 of stabilization of the excited Criegee intermediate under these conditions (Kroll et al., 2001a). Nevertheless, an
28 OH yield of one would still require a reaction time of approximately 0.18 to 0.35 s to produce the observed internal
29 OH concentrations.



1 However, previous measurements have demonstrated that the stabilized Criegee intermediates produced
2 external to the FAGE detection cell from the ozonolysis of propene and (*E*)-2-butene can decompose to produce
3 OH radicals upon entering the low pressure region of the FAGE detection cell (Novelli et al., 2014b). To determine
4 whether the decomposition of stabilized Criegee intermediates are the source of the interference in these
5 experiments, acetic acid was added to the flow tube as an SCI scavenger. Welz et al. (2014) have reported direct
6 measurements of the rate constants for the reactions of CH₂OO and CH₃CHOO Criegee intermediates with formic
7 and acetic acids and found values in excess of $1 \times 10^{-10} \text{ cm}^3 \text{ molecule}^{-1} \text{ s}^{-1}$. Assuming that other Criegee
8 intermediates react similarly, addition of acetic acid should scavenge SCIs in the flow tube. If SCIs are the source
9 of the OH interference, the measured OH signal resulting from addition of acetic acid should be equivalent to the
10 OH signal when the OH interference measured using external C₃F₆ titration is subtracted. The results of these
11 experiments for the ozonolysis of α -pinene and ocimene are shown in Fig. 7. In this figure, the open symbols are
12 the measured OH signal including the interference, while the solid red symbols represent the remaining OH signal
13 after the interference (measured after external C₃F₆ addition) is subtracted. The solid green symbols represent the
14 measured OH signal (without external C₃F₆ addition) when acetic acid is added to the flow tube. As can be seen
15 from this figure, the measured OH signal when acetic acid is added is similar to the OH signal when the
16 interference is subtracted, suggesting that the interference is due to the decomposition of SCIs inside the IU-FAGE
17 detection cell, consistent with the results of Novelli et al. (2014b).

18 The magnitude of the interference observed in these experiments was consistent with the expected
19 steady-state concentration of stabilized Criegee intermediates in the flow tube determined from a chemical model
20 of the ozonolysis of α -pinene using the Master Chemical Mechanism, (MCM v3.2, Jenkin et al., 1997; Saunders
21 et al., 2003). Under the conditions of these experiments, the model predicts a steady-state concentration of
22 stabilized Criegee intermediates (APINBOO) of approximately $2\text{--}6 \times 10^8 \text{ molecules cm}^{-3}$ (Fig. 7). Based on these
23 results, the observed OH interference in these experiments could be explained if approximately 5% of these
24 intermediates dissociated and produced OH radicals inside the IU-FAGE detection cell. In contrast, the MCM
25 predicted steady-state concentration of excited Criegee radicals (APINOOA and APINOOB) in the flow tube was
26 calculated to be on the order of $10^3 \text{ molecules cm}^{-3}$, much less than the observed interference.

27 However, these results are in contrast to the results of Fuchs et al. (2016), who found that in their
28 ozonolysis experiments that the addition of SO₂ as a scavenger for Criegee intermediates did not affect the
29 observed OH signal. They concluded that SCIs were not the cause of the interference in their instrument, although
30 they could not rule out that the interference was due to the decomposition of particular SCI isomers that did not
31 react with SO₂ (Fuchs et al., 2016). These results also appear to be consistent with the observations by Hard et al.



(2002), who found that an interference associated with their alkene ozonolysis calibration experiments disappeared in the presence of 1% water vapor. Given the potentially rapid reaction of Criegee intermediates with water vapor (Chao et al., 2015), this suggests that the source of their interference was also the decomposition of Criegee intermediates inside their detection cell. These results also imply that using the ozonolysis of alkenes as a potential source for calibrating LIF-FAGE instruments may lead to an overestimation of the instrument sensitivity given the potential for this source to produce an interference. However, Dusanter et al. (2008) found that the instrument sensitivities derived from the ozone-alkene calibration technique were systematically lower than those derived from the water-vapor UV- photolysis technique, in contrast to what might be expected if the measurements from the ozonolysis technique were impacted by an interference from Criegee intermediates. But because these ozonolysis experiments were done under humid conditions, it is possible that the Criegee intermediates were scavenged by water vapor prior to entering the IU-FAGE detection cell, thus minimizing the interference.

4. Atmospheric Implications

The percent interference observed in these studies (Figs. S5, S6) is similar to the ambient measurements reported by Mao et al. (2012), who measured an interference that was approximately 50% of the total OH signal in an environment dominated by 2-methyl-3-buten-2-ol (MBO), monoterpenes, sesquiterpenes, and related oxygenated compounds. Novelli et al. (2014a) also found that in their measurements of OH in several forest environments the interference accounted for 30-80% of their total OH signal during the daytime. External addition of SO₂ as an SCI scavenger during some of these measurements resulted in the complete removal of the interference, suggesting that the source of the interference was the decomposition of ambient SCIs inside their detection cell (Novelli et al., 2016). However, the magnitude of the interference signal relative to the calibration for OH was much greater than the expected concentration of SCIs in these environments, which was estimated to be on the order of 5×10^4 molecules cm⁻³ (Novelli et al., 2016). One possible reason for this discrepancy is a greater sensitivity of the LIF-FAGE instrument to the detection of ambient SCIs relative to ambient OH, perhaps due to a greater transmission efficiency of SCIs into the FAGE detection cell. Tests to measure the sensitivity of their LIF-FAGE instrument to the detection of SCIs relative to OH found that the transmission of *syn*-CH₃CHOO through different nozzle designs was different from the transmission of OH radicals (Novelli et al., 2016). These results suggest that the sensitivity of their LIF-FAGE instrument may be different for the detection of SCIs and that using the calibration factor for OH radicals to estimate the SCI concentration from the interference may not be appropriate. However,



1 the sensitivity of their LIF-FAGE instrument to detection of SCIs would have to be a factor of 100 greater than
2 that for OH based on the estimated concentration of ambient SCIs (Novelli et al., 2016).

3 Similar to that observed by Fuchs et al. (2016), extrapolating the interference observed in the experiments
4 presented here as a function of the ozonolysis turnover time (Fig. 6) to concentrations and turnover rates typically
5 observed in the atmosphere (approximately 1.5 ppb hr^{-1} (Hakola et al., 2012; Fuchs et al., 2016)) would suggest
6 that the interference under ambient conditions would be near the detection limit of the IU-FAGE instrument
7 (approximately $4 \times 10^5 \text{ molecules cm}^{-3}$). Consistent with this result, previous measurements of OH radical
8 concentrations by the IU-FAGE instrument in an urban environment during CalNex (California Research at the
9 Nexus of Air Quality and Climate Change) using the external chemical titration technique found no evidence of
10 an unknown interference (Griffith et al., 2016). Measurements of OH by the IU-FAGE instrument in a forested
11 environment in northern Michigan during and after the CABINEX (Community Atmosphere-Biosphere
12 Interactions Experiment) campaign using the external chemical titration technique also did not reveal any
13 unknown interferences (Griffith et al., 2013). However, the measurements during CABINEX were done under
14 relatively cool conditions and low ozone concentrations, where mixing ratios of isoprene were less than 2 ppb and
15 daytime maximum ozone mixing ratios were approximately 30 ppb on average. During CalNex, mixing ratios of
16 isoprene were even lower, less than 1 ppb on average, although maximum daytime mixing ratios of ozone were
17 higher (approximately 50-60 ppb on average during the week and approximately 70-80 ppb on average on the
18 weekends) (Griffith et al., 2016).

19 In contrast, recent measurements of OH concentrations by the IU-FAGE instrument in an Indiana forest
20 using the external chemical titration technique under relatively warmer conditions, with isoprene mixing ratios
21 greater than 4 ppb and higher daytime maximum ozone mixing ratios (approximately 40 ppb) did reveal an
22 interference that correlated with both temperature and ozone concentrations, similar to the results of Mao et al.
23 (2012) (Lew et al., 2017). The magnitude of the observed interference (on the order of $10^6 \text{ molecules cm}^{-3}$) was
24 similar to that observed previously by other LIF-FAGE instruments (Mao et al., 2012; Novelli et al., 2014a; 2016).
25 However, similar to that observed by Novelli et al. (2016), estimates of the ambient concentration of SCIs on the
26 order of approximately $4\text{--}5 \times 10^4 \text{ molecules cm}^{-3}$ for similar environments (Percival et al., 2013; Novelli et al.,
27 2016) suggest that the observed interference in these measurements may not be solely due to ambient SCIs unless
28 there are other significant sources of Criegee radicals that are not accounted for in these models. These results
29 suggest that although SCIs may be contributing to the observed interference, there may exist an unknown
30 interference in these measurements that also correlates with the concentration of ozone and BVOCs (Novelli et
31 al., 2016; Fuchs et al., 2016). Recently, Fuchs et al. (2016) reported an interference in their LIF-FAGE instrument



1 associated with NO₃ radicals, although the exact mechanism of the interference remains unknown. These results
2 suggest that there may be other potential interferences associated with the technique in addition to the
3 decomposition of SCIs that involve complex homogeneous and/or heterogeneous mechanisms inside the FAGE
4 detection cell.

5 **5. Summary and Conclusions**

6 Measurements of OH concentrations produced from the ozonolysis of α -pinene, β -pinene, and ocimene revealed
7 a potential interference associated with the Indiana University LIF-FAGE instrument. The observed interference
8 did not appear to be laser generated and was independent of the ozonolysis reaction time. Addition of acetic acid
9 eliminated the interference, suggesting that the source of the interference in these experiments involved the
10 decomposition of stabilized Criegee intermediates inside the IU-FAGE detection cell. Further measurements and
11 modeling will be needed for a wider variety of alkenes in order to confirm these results.

12 The interference appeared to increase with the length of the inlet in the low pressure region of the
13 detection cell, suggesting that the interference depends on the reaction time in the detection cell. However,
14 increasing the pressure in the detection cell by decreasing the flow rate did not significantly increase the observed
15 interference except for the longest inlet. This may suggest that the increase in the observed interference with the
16 length of the inlet may be the result of increased collisions of the stabilized Criegee intermediates inside the
17 detection cell leading to the formation of OH rather than the result of an increase in reaction time. Additional
18 experiments will be needed to confirm these results. To minimize this potential interference, future measurements
19 of OH by the IU-FAGE instrument will involve a detection cell design that minimizes both reaction time and
20 potential surface collisions.

21 Regardless, future ambient measurements by the IU-FAGE instrument will incorporate the external OH
22 titration technique to quantify these and other potential unknown interferences. Because of differences in design
23 (geometry, cell pressure, flow, etc.) these interference measurements may not apply to other LIF-FAGE
24 instruments. However, it is recommended that future OH measurements using the LIF-FAGE technique
25 incorporate an external OH titration scheme or some other method to quantify potential artefacts.

26
27 Acknowledgements: This work was supported by the National Science Foundation, grants AGS-1104880 and
28 AGS-1440834. We would like to thank Sebastien Dusanter for helpful comments on the manuscript.



References

- Aschmann, S. M., Arey, J., and Atkinson, R.: OH radical formation from the gas-phase reactions of O₃ with a series of terpenes. *Atmos. Environ.*, 36(27), 4347-4355. 2002.
- Atkinson, R., Aschmann, S. M., Arey, J., and Shorees, B.: Formation of OH Radicals in the Gas-Phase Reactions of O₃ with a Series of Terpenes. *J. Geophys. Res. Atmos.*, 97(D5), 6065-6073. 1992.
- Atkinson, R.: Gas Phase Tropospheric Chemistry of Volatile Organic Compounds: 1. Alkanes and Alkenes, *J. Phys. Chem. Ref. Data*, 26, 215, 1997.
- Atkinson, R., Baulch, D. L., Cox, R. A., Crowley, J. N., Hampson, R. F., Hynes, R. G., Jenkin, M. E., Rossi, M. J., Troe, J., and IUPAC Subcommittee: Evaluated kinetic and photochemical data for atmospheric chemistry: Volume II – gas phase reactions of organic species, *Atmos. Chem. Phys.*, 6, 3625-4055, 2006.
- Chao, W., Hsieh, J.-T., Chang, C.-H., and Lin, J. J.-M.: Direct kinetic measurement of the reaction of the simplest Criegee intermediate with water vapor, *Science*, 347, 751-754, 2015.
- Chew, A. A., and Atkinson, R.: OH radical formation yields from the gas-phase reactions of O₃ with alkenes and monoterpenes. *J. Geophys. Res. Atmos.*, 101(D22), 28649-28653. 1996.
- Dusanter, S., Vimal, D., and Stevens, P. S.: Technical note: Measuring tropospheric OH and HO₂ by laser-induced fluorescence at low pressure. A comparison of calibration techniques. *Atmos. Chem. Phys.*, 8(2), 321-340. 2008.
- Dusanter, S., Vimal, D., Stevens, P. S., Volkamer, R., Molina, L. T., Baker, A., Meinardi, S., Blake, D., Sheehy, P., Merten, A., Zhang, R., Zheng, J., Fortner, E. C., Junkermann, W., Dubey, M., Rahn, T., Eichinger, B., Lewandowski, P., Prueger, J., and Holder, H.: Measurements of OH and HO₂ Concentrations during the MCMA-2006 Field Campaign: Part 2 – Model Comparison and Radical Budget, *Atmos. Chem. Phys.*, 9, 6655-6675, 2009.
- Faloona, I., Tan, D., Brune, W., Hurst, J., Barket, D., Couch, T. L., Shepson, P., Apel, E., Riemer, D., Thornberry, T., Carroll, M. A., Sillman, S., Keeler, G. J., Sagady, J., Hooper, D., and Paterson, K.: Nighttime observations of anomalously high levels of hydroxyl radicals above a deciduous forest canopy. *J. Geophys. Res. Atmos.*, 106(D20), 24315-24333. 2001.
- Fuchs, H., Tan, Z., Hofzumahaus, A., Broch, S., Dorn, H.-P., Holland, F., K \ddot{u} nstler, C., Gomm, S., Rohrer, F., Schrader, S., Tillmann, R., and Wahner, A.: Investigation of potential interferences in the detection of atmospheric ROx radicals by laser-induced fluorescence under dark conditions, *Atmos. Meas. Tech.*, 9, 1431-1447. 2016.



- Griffith, S. M., Hansen, R. F., Dusanter, S. Stevens, P. S., Alaghmand, M., Bertman, S. B., Carroll, M. A., Erickson, M., Galloway, M., Grossberg, N., Hottle, J., Hou, J., Jobson, B. T., Kammrath, A., Keutsch, F. N., Lefer, B. L., Mielke, L. M., O'Brien, A., Shepson, P. B., Thurlow, M., Wallace, W., Zhang, N., Zhou, X., L.: OH and HO₂ radical chemistry during PROPHET 2008 and CABINEX 2009 – Part 1: Measurements and model comparison, *Atmos. Chem. Phys.*, 13, 5403–5423, 2013.
- Griffith, S. M., Hansen, R. F., S. Dusanter, Michoud, V., Gilman, J. B., Kuster, W. C., Veres, P. R., Graus, M., de Gouw, J. A., Roberts, J., Young, C., Washenfelder, R., Brown, S. S., Thalman, R., Waxman, E., Volkamer, R., Tsai, C., Stutz, J., Flynn, J. H., Grossberg, N., Lefer, B., Alvarez, S. L., Rappenglueck, B., Mielke, L. H., Osthoff, H. D., and Stevens, P. S.: Measurements of hydroxyl and hydroperoxy radicals during CalNex-LA: Model comparisons and radical budgets, *J. Geophys. Res. Atmos.*, 121, 4211–4232. 2016.
- Hakola, H., Hellén, H., Hemmilä, M., Rinne, J., and Kulmala, M.: In situ measurements of volatile organic compounds in a boreal forest, *Atmos. Chem. Phys.*, 12, 11665–11678, 2012.
- Hansen, R. F., Griffith, S. M., Dusanter S., Rickly, P. S., Stevens, P. S., Bertman, S. B., Carroll, M. A., Erickson, M. H., Flynn, J. H., Grossberg, N., Jobson, B. T., Lefer, B. L., and Wallace, H. W. Measurements of total hydroxyl radical reactivity during CABINEX 2009 – Part 1: field measurements. *Atmos. Chem. Phys.*, 14(6), 2923–2937. 2014.
- Hard, T. M., George, L. A. and O'Brien, R. J.: An Absolute Calibration for Gas-Phase Hydroxyl Measurements. *Environ. Sci. Technol.* 36, 1783–1790, 2002.
- Heard, D. E. and Pillings, M. J.: Measurement of OH and HO₂ in the Troposphere. *Chem. Rev.*, 103 (12), 5163–5198. 2003.
- Hofzumahaus, A., Rohrer, F., Lu, K., Bohn, B., Brauers, T., Chang, C.-C., Fuchs, H., Holland, F., Kita, K., Kondo, Y., Li, X., Lou, S., Shao, M., Zeng, L., Wahner, A., and Zhang, Y.: Amplified Trace Gas Removal in the Troposphere. *Science*, 324(5935), 1702–1704. 2009.
- Jenkin, M. E., Saunders, S. M., and Pilling, M. J.: The tropospheric degradation of volatile organic compounds: a protocol for mechanism development, *Atmos. Environ.*, 31, 81–104. 1997.
- Kroll, J. H., Clarke, J. S., Donahue, N. M., Anderson, J. G., and Demerjian, K. L.: Mechanism of HO_x formation in the gas-phase ozone-alkene reaction. 1. Direct, pressure-dependent measurements of prompt OH yields. *J. Phys. Chem. A*, 105(9), 1554–1560. 2001a.
- Kroll, J. H., Sahay, S. R., Anderson, J. G., Demerjian, K. L., and Donahue, N. M.: Mechanism of HO_x Formation in the Gas-Phase Ozone-Alkene Reaction. 2. Prompt versus Thermal Dissociation of Carbonyl Oxides to Form OH. *J. Phys. Chem. A*, 105 (18), 4446–445, 2001b.



- Lelieveld, J., Butler, T. M., Crowley, J. N., Dillon, T. J., Fischer, H., Ganzeveld, L., Harder, H., Lawrence, M. G., Martinez, M., Taraborrelli, D. and Williams, J.: Atmospheric oxidation capacity sustained by a tropical forest, *Nature*, 452, 737-740, 2008.
- Lew, M., Sigler, P., Bottorff, B., Sklaveniti, S., Léonardis, T., Locoge, N. Dusanter, S., Kundu, S., Deming, B., Wood, E., and Stevens, P.S.: HO_x Radical Chemistry in an Indiana Forest: Measurement and Model Comparison, in preparation, 2017.
- Mao, J., Ren, X., Zhang, L., Van Duin, D. M., Cohen, R. C., Park, J. H., Goldstein, A. H., Paulot, F., Beaver, M. R., Crounse, J. D. Wennberg, P. O. DiGangi, J. P., Henry, S. B., Keutsch, F. N., Park, C., Schade, G. W., G. M. Wolfe, G. M., Thornton, J. A. and Brune, W. H.: Insights into hydroxyl measurements and atmospheric oxidation in a California forest. *Atmos. Chem. Phys.*, 12(17), 8009-8020. 2012.
- Novelli, A., Hens, K., Tatum Ernest, C., Kubistin, D., Regelin, E., Elste, T., Plass-Dülmer, C., Martinez, M., Lelieveld, J., and Harder, H.: Characterisation of an inlet pre-injector laser-induced fluorescence instrument for the measurement of atmospheric hydroxyl radicals, *Atmos. Meas. Tech.*, 7, 3413-3430. 2014a.
- Novelli, A., Vereecken, L., Lelieveld, J., and Harder, H.: Direct observation of OH formation from stabilised Criegee intermediates, *Phys. Chem. Chem. Phys.*, 16, 19941–19951, 2014b.
- Novelli, A., Hens, K., Tatum Ernest, C., Martinez, M., Nölscher, A. C., Sinha, V., Paasonen, P., Petäjä, T., Sipilä, M., Elste, T., Plass-Dülmer, C., Phillips, G. J., Kubistin, D., Williams, J., Vereecken, L., Lelieveld, J., and Harder, H.: Identifying Criegee intermediates as potential oxidants in the troposphere, *Atmos. Chem. Phys. Discuss.*, doi:10.5194/acp-2016-919, in review, 2016.
- Percival, C. J., Welz, O., Eskola, A. J., Savee, J. D., Osborn, D. L., Topping, D. O., Lowe, D., Utembe, S. R., Bacak, A., McFiggans, G., Cooke, M. C., Xiao, P., Archibald, A. T., Jenkin, M. E., Derwent, R. G., Riipinen, I., Mok, D. W., Lee, E. P., Dyke, J. M., Taatjes, C. A., and Shallcross, D. E.: Regional and global impacts of Criegee intermediates on atmospheric sulphuric acid concentrations and first steps of aerosol formation, *Faraday Discuss.*, 165, 45-73. 2013.
- Ren, X. R., Harder, H., Martinez, M., Faloona, I. C., Tan, D., Leshner, R. L., Di Carlo, P. Simpas, J. B., and Brune, W. H.: Interference testing for atmospheric HO_x measurements by laser-induced fluorescence. *J. Atmos. Chem.*, 47(2), 169-190. 2004.
- Ren, X., Olson, J. R., Crawford, J. H., Brune, W. H., Mao, J., Long, R. B., Chen, A., Chen, G., Avery, M. A., Sachse, G. W., Barrick, J. D., Diskin, Huey, L. G., Fried, A., Cohen, R. C., Heikes, B., Wennberg, P. O., Singh, H. B., Blake, D. R., and Shetter, R. E.: HO_x chemistry during INTEX-A 2004: Observation, model



- calculation, and comparison with previous studies, *J. Geophys. Res.*, 113, D05310, doi:10.1029/2007JD009166, 2008.
- Rohrer, F., Lu, K., Hofzumahaus, A., Bohn, B., Brauers, T., Chang, C.-C., Fuchs, H., Haseler, R., Holland, F., Hu, M., Kita, K., Kondo, Y., Li, X., Lou, S., Oebel, A., Shao, M., Zeng, L., Zhu, T., Zhang, Y., and Wahner, A.: Maximum efficiency in the hydroxyl-radical-based self-cleansing of the troposphere, *Nature Geosci.*, 7, 559-563, 2014.
- Tan, D., Faloon, I., Simpas, J. B., Brune, W., Shepson, P. B., Couch, T. L., Sumner, A. L., Carroll, M. A., Thornberry, T., Apel, E., Riemer, D., and Stockwell, W.: HO_x budgets in a deciduous forest: Results from the PROPHET summer 1998 campaign. *J. Geophys. Res. Atmos.*, 106(D20), 24407-24427. 2001.
- Saunders, S. M., Jenkin, M. E., Derwent, R. G., and Pilling, M. J.: Protocol for the development of the Master Chemical Mechanism, MCM v3 (Part A): tropospheric degradation of non-aromatic volatile organic compounds. *Atmos. Chem. Phys.*, 3, 161-180. 2003.
- Siese, M., Becker, K.H., Brockmann, K.J., Geiger, H., Hofzumahaus, A., Holland, F., Mihelcic, D., Wirtz, K., Direct measurement of OH radicals from ozonolysis of selected alkenes: a EUPHORE simulation chamber study. *Environ. Sci. Technol.*, 35, 4660–4667, 2001.
- Schlosser, E., Bohn, B., Brauers, T., Dorn, H.-P., Fuchs, H., Häseler, R., Hofzumahaus, A., Holland, F., Rohrer, F., Rupp, L. O., Siese, M., Tillmann, R., and Wahner, A.: Intercomparison of Two Hydroxyl Radical Measurement Techniques at the Atmosphere Simulation Chamber SAPHIR. *J. Atmos. Chem.*, 56(2), 187-205. 2007.
- Schlosser, E., Brauers, T., Dorn, H.-P., Fuchs, H., Häseler, R., Hofzumahaus, A., Holland, F., Wahner, A., Kanaya, Y., Kajii, Y., Miyamoto, K., Nishida, S., Watanabe, K., Yoshino, A., Kubistin, D., Martinez, M., Rudolf, M., Harder, H., Berresheim, H., Elste, T., Plass-Dülmer, C., Stange, G., and Schurath, U.: Technical Note: Formal blind intercomparison of OH measurements: results from the international campaign HO_xComp, *Atmos. Chem. Phys.*, 9, 7923-7948, 2009.
- Stevens, P. S., Mather, J. H., Brune, W. H.: Measurement of tropospheric OH and HO₂ by laser-induced fluorescence at low pressure. *J. Geophys. Res.*, 99, 3543-3557, 1994.
- Welz, O., Eskola, A. J., Sheps, L., Rotavera, B., Savee, J. D., Scheer, A. M., Osborn, D. L., Lowe, D., Murray Booth, A., Xiao, P., Anwar H. Khan, M., Percival, C. J., Shallcross, D. E. and Taatjes, C. A.: Rate Coefficients of C1 and C2 Criegee Intermediate Reactions with Formic and Acetic Acid Near the Collision Limit: Direct Kinetics Measurements and Atmospheric Implications. *Angew. Chem. Int. Ed.*, 53, 4547–4550. 2014.

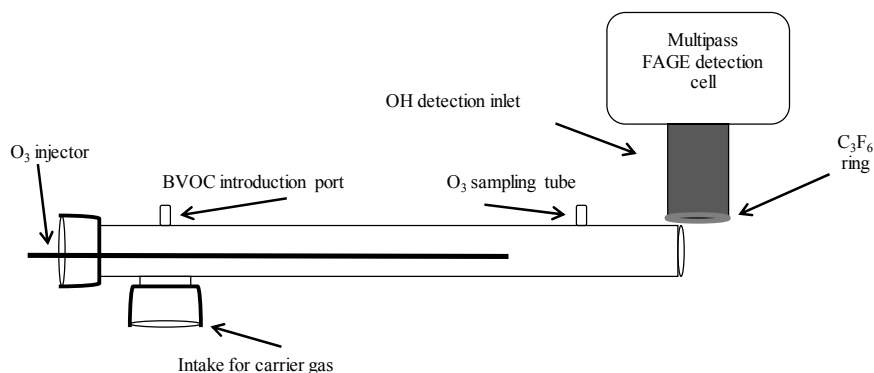


Figure 1: Schematic of the atmospheric pressure flow system used in this study.

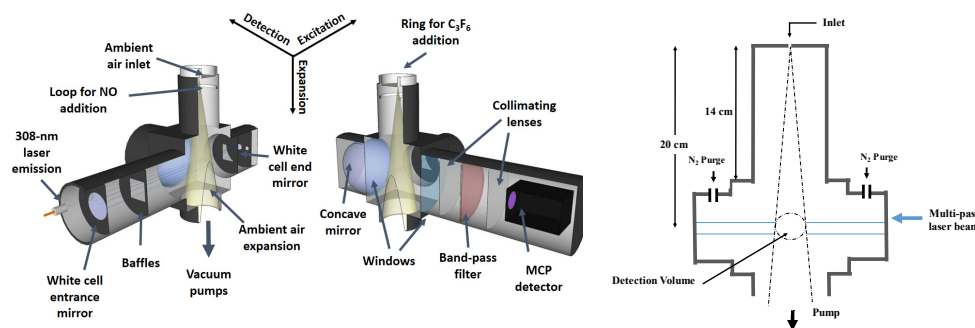


Figure 2. Schematic of the IU-FAGE sampling/excitation axis (left) and cross section with dimensions for the medium inlet configuration (right).

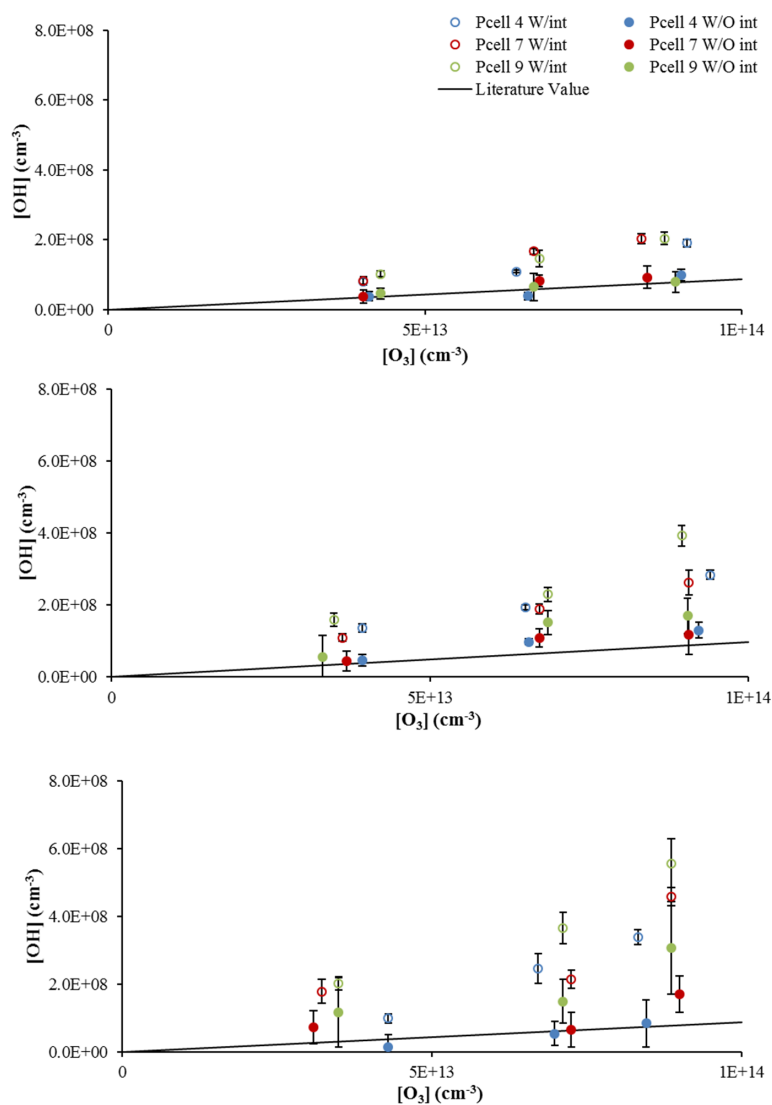


Figure 3. OH concentrations from α -pinene ozonolysis at three cell pressures with and without the interference using the 0.6 mm diameter nozzle and the short (top), medium (middle), and long (bottom) inlet lengths with α -pinene concentrations of approximately $3 \times 10^{12} \text{ cm}^{-3}$. Error bars indicate the precision of the measurement (1σ). Lines indicate the expected steady-state OH concentration based on published values of the OH yield (see text).

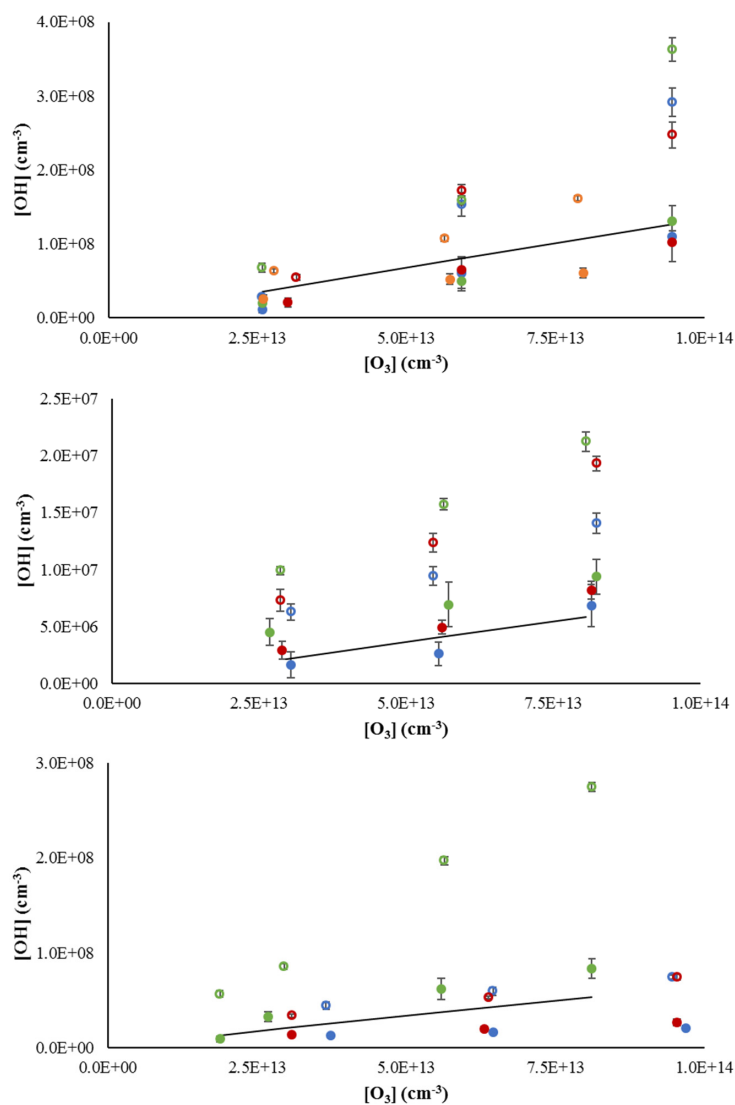


Figure 4. OH concentrations using the short inlet from the ozonolysis of α -pinene (top, 1×10^{12} – 4×10^{13} cm⁻³), β -pinene (middle, 1×10^{11} – 4×10^{13} cm⁻³), and ocimene (bottom, 2×10^{11} – 5×10^{13} cm⁻³). Open circles indicate measurements with the interference, filled circles without the interference. Colors indicate relative concentrations (orange>green>red>blue). Solid lines reflect the expected OH radical yield (see text). Error bars reflect the measurement precision (1σ).

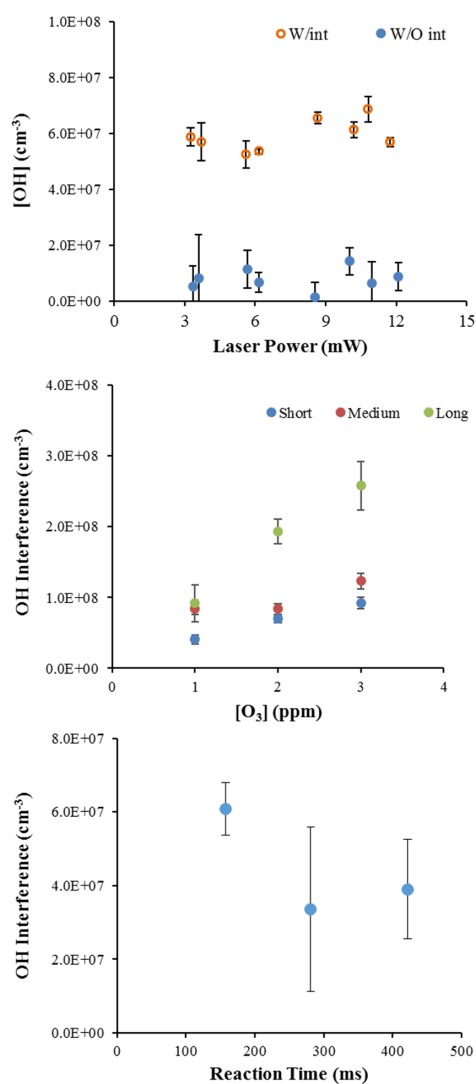


Figure 5. OH concentrations from ocimene ozonolysis with varied laser power at an ozone mixing ratio of 2 ppm and ocimene concentration of approximately $3 \times 10^{13} \text{ cm}^{-3}$ (top). OH interference during α -pinene ozonolysis based on ozone concentration and inlet length with an α -pinene concentration of approximately $3 \times 10^{12} \text{ cm}^{-3}$ (middle). OH interference measurements during ocimene ozonolysis as a function of reaction time with an ocimene concentration of approximately $3 \times 10^{13} \text{ cm}^{-3}$ (bottom).

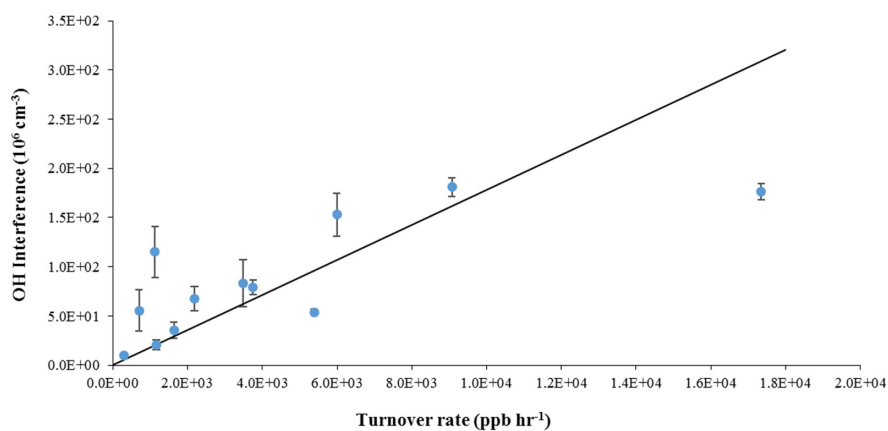


Figure 6. Interference signal as a function of turnover rate for the ozonolysis of α -pinene using the short inlet. Solid line reflects the slope observed by Fuchs et al. (2016).

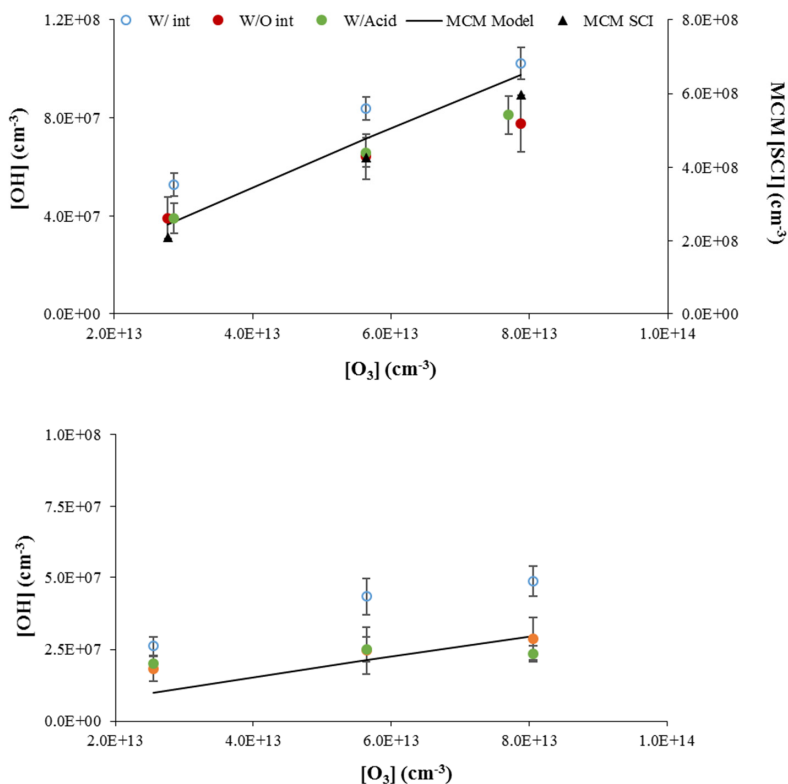


Figure 7. Measurements of OH concentrations from the ozonolysis of α -pinene (approximately $1 \times 10^{12} \text{ cm}^{-3}$, top) and ocimene (approximately $4 \times 10^{11} \text{ cm}^{-3}$, bottom). Open symbols are measurements including the interference, filled red circles are the resulting OH measurements when the interference determined by C₃F₆ addition is subtracted, and the filled green circles are the OH measurements when acetic acid is added to the flow tube. The lines indicate the expected OH concentration from published OH yields. The black triangles in the top plot reflect the predicted concentration of stabilized Criegee intermediates by the Master Chemical Mechanism (see text).